IEEE Access
Multidisciplinary | Rapid Review | Open Access Journal

Received January 7, 2020, accepted January 23, 2020, date of publication January 28, 2020, date of current version February 6, 2020.

Digital Object Identifier 10.1109/ACCESS.2020.2970064

Pulse Width Tuning in Electrochemical Micro-Machining System

CHUANJUN ZHAO AND LIZHONG XU
Mechanical Engineering School, Yanshan University, Qinhuangdao 066004, China
Corresponding author: Lizhong Xu (xlz@ysu.edu.cn)

ABSTRACT In electrochemical micro-machining technology using ultra-short pulses, the machining accuracy is limited by pulse width of the power supply. Here, a mathematical model for tuning pulse width in electrochemical micro machining by means of differential circuits was proposed. Using this model, the step responses of the system under different time constants were simulated, which showed that the pulse width of the step response becomes quite short when the time constant of the differential circuit is short enough. Based on the model, an electrochemical micro-machining system was produced. Using this system, some micro-structures were successfully produced. The machining accuracy reaches the nanometer scale. This illustrates our model for tuning pulse width in electrochemical micro machining.

INDEX TERMS Electrochemistry, differential circuit, micro-machining, pulse width tuning.

I. INTRODUCTION

Electrochemical theory is used widely in chemical power, sensors, biological signal analysis and micro machining [1]–[5]. The electrochemical system is a coupled electronic and ion circuit system. The performance of the electrochemical system is determined by the coupled electronic-ion circuit.

Using the electrochemical theories, a series of immune-sensors, enzyme sensors and DNA sensors were proposed and these biological processes were investigated in details [6]–[10]. The electrochemical theories are also used to model electrochemical systems for many ion batteries and the operating performance of the batteries was improved significantly [11]–[14]. The electrochemical theories are also used for electrochemical treatment in the local control of solid tumors in preclinical and clinical studies [15], [16].

R. Schuster used an equivalent circuit model to describe the coupled electronic and ion circuit for the electrochemical micromachining and proposed electrochemical micro-machining (ECM) technique using ultra short pulses [17]. The technique increased machining resolution of the micro structures significantly and has received extensive attention in the world [18]–[23].

Typical micro-nano electromechanical systems include micro-nano motors, sensors, and fluid devices, etc. The corresponding micro-nano manufacturing technologies include ultrasonic machining technology [24], laser machining technology [25], EDM technology [26], and electrochemical machining technology [27]. Among them, electrochemical machining technology has high machining efficiency for conductor materials and plays an important role in manufacturing various micro-nano structures.

Although the precision of micro-ECM can be greatly improved by using ultra-short pulse signals, the machining accuracy is limited by the pulse power supply. The pulse width of voltage signals produced by the power supply has not been reduced without limitation. In addition, the cost of ultra-short pulse power supply is high and difficult to be widely used in practical production. It is because the step signal of ultra-short pulse width is used in the above micro-ECM technology, the shorter the pulse width of the step signal, the higher the requirement for power supply.

In order to solve the above problems, this paper puts forward a mathematical model for tuning pulse width of the voltage signals by means of the differential circuits in the micro-ECM. Using the model, the step responses of the system under different time constants are simulated, which shows that the pulse width of the step response becomes quite short when the time constant of the differential circuit is short enough. Based on it, stray corrosion in micro-ECM is investigated and the system time constant corresponding to the best localization of micro-ECM is determined. Based on the model, an electrochemical micro machining system is produced. Using this system, some micro-structures such

The associate editor coordinating the review of this manuscript and approving it for publication was Abdallah Kassem.

as the micro-cantilever beam and the micro-curved beam are successfully produced. The machining accuracy reaches the nanometer scale. Here, the ultra-short pulse signals are generated by ordinary step signals plus a differential circuit, so there is no special requirement for expensive power supply. This illustrates our mathematical model for tuning pulse width in electrochemical micro machining.

II. CONTROL EQUATION AND PULSE WIDTH TUNING BASED ON ONE DIFFERENTIAL CIRCUIT

On the basis of the existing rectangular pulse ECM circuit, a differential circuit is introduced, and the conventional rectangular pulse signal is transformed into a tip pulse signal, which is more suitable for ECM. The characteristic of the differential circuit is related to its time constant τ ($\tau = RC$). The smaller is the time constant, the shorter the charge and discharge time on the electric poles. Here, the tip pulse of the output end of the differential circuit is used for ECM. In order to improve the accuracy of ECM, the differential circuit is required to have a rapid charge and discharge speed. Therefore, the time constant of the differential circuit should be as small as possible.

When the time constant of the differential circuit is given, the rectangular pulse voltage signal is used as the input, and then the output voltage waveform has positive and negative peaks. In ECM, the workpiece is connected to the positive pole of the power source so that its metal atoms lose electrons in the oxidation reaction. The tool is connected to the negative electrode of the power source and the hydrogen ions on the negative electrode surface receive electrons during the reduction reaction.

At the moment when the rectangular pulse signals drop, the reverse voltage output from the *RC* differential circuit will lead to reverse ECM. Therefore, the reverse voltage of the output of the RC differential circuit must be eliminated. For this purpose, a simple single-phase half-wave rectifier circuit is introduced to filter the reverse voltage signal.

By introducing the RC differential circuit into the equivalent circuit of micro-ECM, the equivalent circuit diagram of the micro-ECM system with the differential circuit can be obtained, as shown in figure 1. Since the single-phase rectifier circuit has no effect on the time-domain response of the machining system, it is ignored in the theoretical analysis.

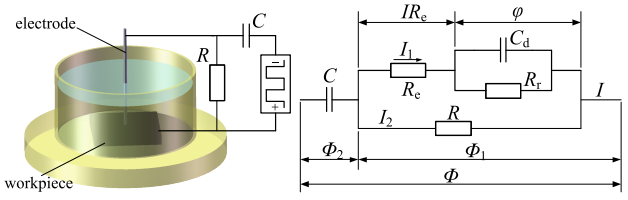

FIGURE 1. Equivalent circuit of the micro-ECM system with differential circuit.

In Fig. 1, I is the total current, I_1 is the electrolyte circuit current, and I_2 is the resistive current in the differential circuit; Φ is the pulse voltage of the power supply, Φ_1 is the voltage between the positive and negative electrodes of the electrochemical reaction, Φ_2 is the voltage on the capacitance of the differential circuit, and φ is the voltage on the double layer capacitance on the electrode surface; R is the differential circuit resistance, R_e is the electrolyte resistance, and R_r is the electrochemical reaction resistance; C is the differential circuit capacitance, C_d is the double layer capacitance on the electrode surface.

From Fig.1, we know

$$I_1 = C_d \frac{d\varphi}{dt} + \frac{\varphi}{R_r} \tag{1}$$

where t is the time.

The reaction resistance R_r is very large. The current component on it can be neglected. Thus

$$I_1 = C_d \frac{d\varphi}{dt} \tag{2}$$

From circuit Ohm's law, we obtain

$$\Phi_1 = R_e C_d \frac{d\varphi}{dt} + \varphi \tag{3}$$

$$I_2 = \frac{\Phi_1}{R} = \frac{R_e C_d}{R}\frac{d\varphi}{dt} + \frac{\varphi}{R} \tag{4}$$

$$I = C\frac{d\Phi_2}{dt} \tag{5}$$

Considering $I = I_1 + I_2$, and combining Eqs. (2), (4) and (5), yields

$$C\frac{d\Phi_2}{dt} = C_d \frac{d\varphi}{dt} + \frac{R_e C_1}{R}\frac{d\varphi}{dt} + \frac{\varphi}{R} \tag{6}$$

Doing Laplace transform to Eq. (6), yields

$$Cs\Phi_2(s) = \frac{R + R_e}{R} C_d s\varphi(s) + \frac{1}{R}\varphi(s) \tag{7}$$

From Fig. 1, it is also known

$$\Phi = \Phi_1 + \Phi_2 = R_e C_d \frac{d\varphi}{dt} + \varphi + \Phi_2 \tag{8}$$

Doing Laplace transform to Eq. (8), yields

$$\Phi(s) = R_e C_d s\varphi(s) + \varphi(s) + \Phi_2(s) \tag{9}$$

Combining Eq. (7) with (9), yields

$$G(s) = \frac{\varphi(s)}{\Phi(s)} = \frac{RCs}{RR_e C_d C s^2 + (RC_d + R_e C_d + RC)s + 1} \tag{10}$$

From Eg. (10), we can obtain the Laplace transform of the system response to unit step voltage

$$C(s) = G(s)R(s) = \frac{RC}{RR_e C_d C s^2 + (RC_d + R_e C_d + RC)s + 1} \tag{11}$$

The unit step time response of the system is obtained by inverse Laplace transform

$$\varphi(t) = \frac{RC\omega_n}{\sqrt{1-\xi^2}} e^{-\xi\omega_n t} \sin\omega_n \sqrt{1-\xi^2}\, t \tag{12}$$

where ξ is the damping factor of the system, ω_n is its natural frequency.

$$\xi = \frac{RC_d + R_eC_d + RC}{\sqrt{RR_eC_dC}} \tag{13}$$

$$\omega_n = \frac{1}{\sqrt{RR_eC_dC}} \tag{14}$$

The double layer capacitance on the electrode surface $C_d = C_pS$, C_p = 20-50 μF/cm^2, it is DL capacitance per unit area; S is effective area for the electrode to participate in the reaction; for the tool pole 10μm in diameter, $S \approx 7.85\times10^{-7}$cm^2. So, we know that $C_d \approx (1.57\text{-}3.93)\times10^{-5}\mu$F. Usually, the differential circuit capacitance is taken to be 0.01-1μF. From these data, we know that $RC_d \ll RC$ and RC_d could be neglected. Thus, the damping factor of the system can be given by

$$\xi = \frac{R_eC_d + \tau}{\sqrt{R_eC_d\tau}} \tag{15}$$

From constant inequality, $a + b \geq 2\sqrt{ab}$, it is known

$$R_eC_d + \tau > \sqrt{R_eC_d\tau} \tag{16}$$

Hence, the damping factor $\xi > 1$ and the system is an over-damped second-order system. The unit step response of the system is

$$\varphi(t) = \frac{RC\omega_n}{\sqrt{\xi^2-1}}e^{-\xi\omega_n t}\sin\omega_n\sqrt{\xi^2-1}t \tag{17}$$

When the process parameters (electrode diameter, electrolyte type, and electrolyte concentration) are determined, the electrolyte resistance (R_e) and double layer capacitance (C_d) are both fixed constants. Therefore, the step response of the ECM system with the differential circuit is only related to the time constant τ of the differential circuit. Using Eq. (17), the step responses of the system under different time constants are simulated (see Fig. 2). In order to facilitate the comparison of the same processing test, the tool electrode diameter is taken to be 10 μm. Fig. 2 shows:

With the decrease of the time constant τ, the charge and discharge times of the differential circuit decrease, and the peak response time and the peak voltage of the system also decrease. Therefore, the smaller the time constant τ of the differential circuit, the better the precision of ECM. However, the smaller is the time constant τ, the smaller the corresponding peak voltage φ_{max}. The peak voltage φ_{max} on the double layer must be larger than the decomposing voltage φ_d of the workpiece in order to ensure the normal process of ECM, that is, $\varphi_{max} \geq \varphi_d$. Therefore, it is necessary to adjust the input voltage of the pulse power supply.

According to Eq. (17), the peak time t_p of the step response is

$$t_p = \frac{\text{arc cot}\frac{\xi}{\sqrt{\xi^2-1}}}{\omega_n\sqrt{\xi^2-1}} \tag{18}$$

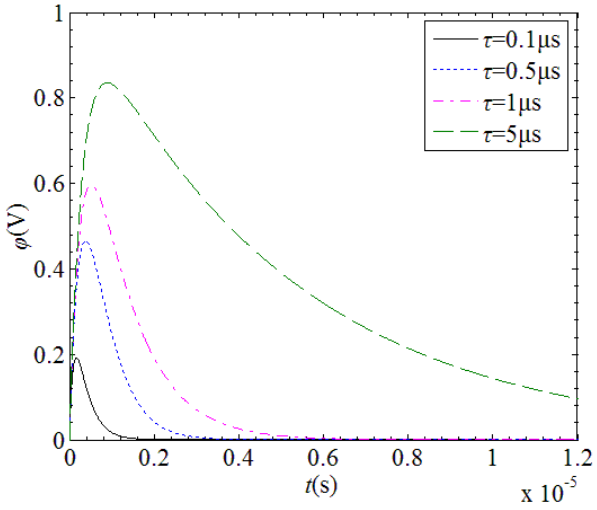

FIGURE 2. Step response of the system for different τ.

The peak voltage of the response is

$$\varphi_{max} = \varphi(t_p) = \frac{RC\omega_n}{\sqrt{\xi^2-1}}e^{-\xi\omega_n t_p}\sin\omega_n\sqrt{\xi^2-1}t_p \tag{19}$$

In order for the peak voltage of the step response to reach the decomposition voltage of the workpiece, it is necessary to modify the voltage of the pulse power supply. The modified peak voltage is

$$\varphi'_{max} = K\varphi_{max} \tag{20}$$

where K is the modified factor.

Combining Eq. (20) and the decomposition condition $\varphi'_{max} \geq \varphi_d$, we obtain

$$K \geq \frac{\varphi_d}{\varphi_{max}} \tag{21}$$

Take the decomposition voltage to be $\varphi_d = 0.85$ V and combine Eqs. (18) and (19) with (21), the minimum modified factor K of the pulse power supply under different time constants τ is calculated (see Fig. 3a). As can be seen from the figure:

With the increase of the time constant τ, the coefficient K decreases sharply, and then gradually tends to 1. This is because the larger the time constant τ, the slower the charge of the capacitor, and more voltage of the pulse power supply is applied to both ends of the resistance R. The output voltage of the differential circuit is basically the same as the input voltage of the pulse power supply.

When the differential circuit time constant $\tau = 0.5$ μs, the corresponding minimum modified factor (K) of the power supply voltage is 1.83. That is, the peak voltage of the step response of the system will be greater than the decomposition voltage φ_d of ECM if the voltage of the pulse power supply is greater than 1.83 φ_d. According to Fig. 3a, we determine the modified factor for different time constants, and then the step responses for the modified voltages are simulated as shown in Fig. 3b. It shows:

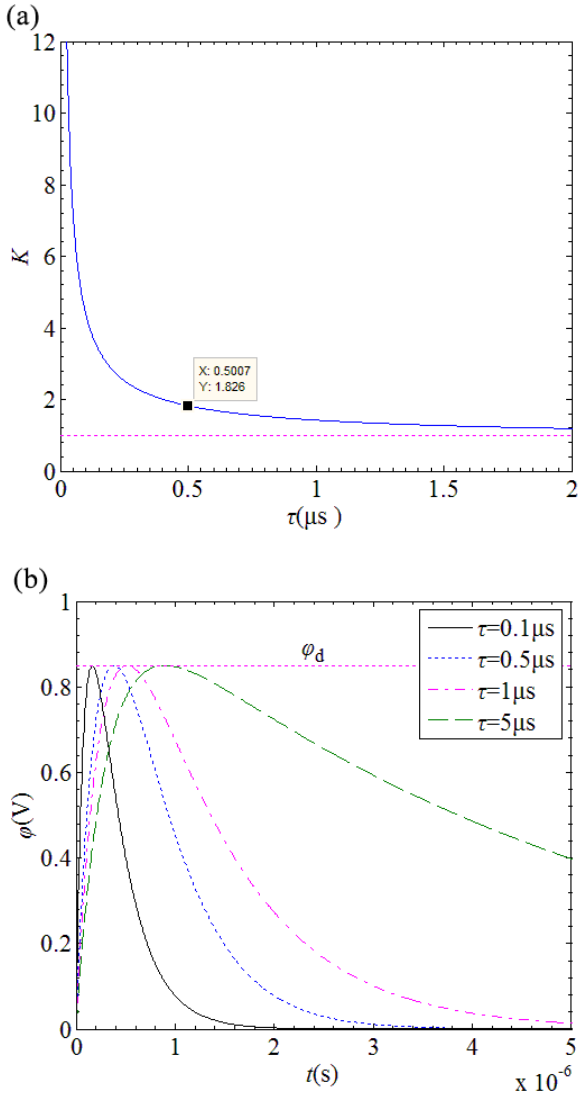

FIGURE 3. Modified factor K and step response after modification. a) K changes with τ; b) step response after modification.

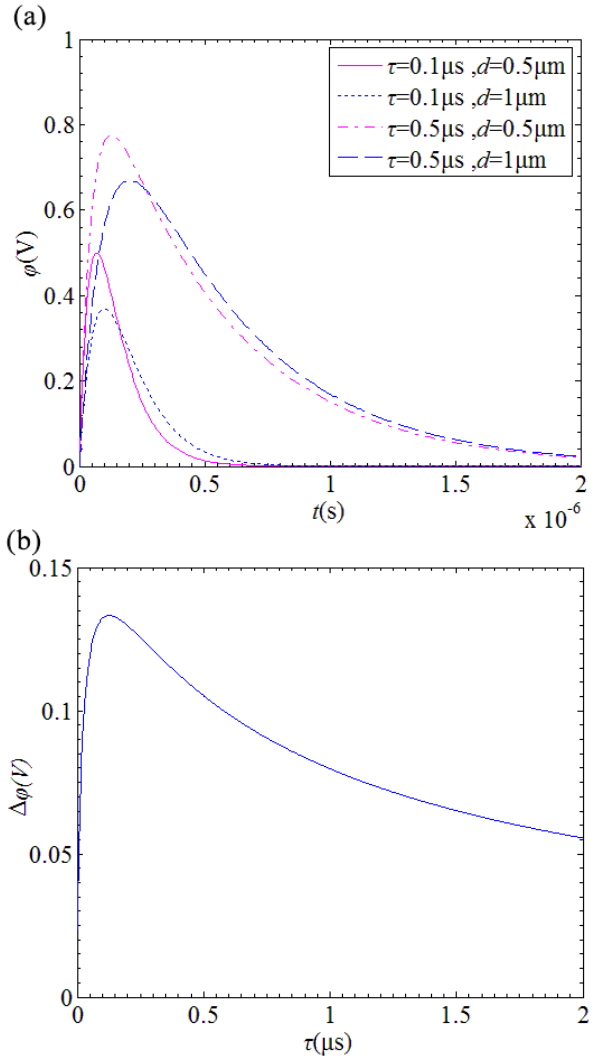

FIGURE 4. Step responses and $\Delta\varphi$ changes of the system. a) step responses of the system; b) $\Delta\varphi$ changes along with τ.

As the time constant τ of the differential circuit changes, the peak voltage of the step response of the system can be guaranteed to be exactly equal to the decomposing voltage of the workpiece by adjusting the output voltage of the pulse power supply. When the time constant $\tau = 0.5\ \mu$s, the peak response time of the system is about 383 ns.

Stray corrosion in ECM mainly refers to the phenomenon that the non-machined area far away from the electrode is corroded and it is the main factor that affects the precision of ECM. In electrochemical machining of micro-holes, the dimension precision of micro-hole diameter is determined by the machined side gap between the tool and workpiece, which is the direct reflection of the localization of electrolytic machining. Therefore, it is representative to study the localization of the machining method by machining micro-holes.

According to the effect of electrode steady-state potential on ECM under different pulse conditions, we know that if the electrode potential in machining area can exceed the decomposition potential of anodic metal, the electrode potential in non-machined area is lower than the decomposition potential, the electrochemical reaction can only occur in the processing zone, and there is no electrochemical reaction in the non-processing zone. That is, only the material in the processing zone is dissolved and corroded, which could greatly improve the localization of ECM. According to the mathematical model of real pulse ECM system based on differential circuit, the step response of the system with different time constants τ and clearance d between the workpiece and tool is simulated. The results are shown in Fig. 4a. It shows:

The smaller is the clearance d, the greater the peak voltage of the system response when the time constant τ of the differential circuit is the same. When the clearance is 0.5 μm and 1 μ m, the difference of corresponding peak voltage $\Delta\varphi$ could reflect the localization of ECM. The larger is $\Delta\varphi$, the lower is the voltage at the place far from the electrode,

the weaker is the electrochemical reaction and the better is the localization of ECM. Therefore, we can approximately describe the localization of ECM by using the difference of peak voltage $\Delta\varphi$. Because the time constant of differential circuit has a main effect on the step response of the system, the localization of ECM is different under different time constants. In order to increase the precision of ECM as highly as possible, a time constant value of differential circuit should be found where the corresponding peak voltage difference $\Delta\varphi$ is maximized.

Taking the time constant τ of differential circuit as variable, the peak voltage of system response is calculated when the distance between poles is 0.5 μm and 1 μm. The difference $\Delta\varphi$ between the two voltages is obtained (see Fig.4b). It shows:

With the increase of the time constant τ, the voltage difference $\Delta\varphi$ increases sharply at first and then decreases slowly. When the time constant increases to close to the pulse duration t_{on}, $\Delta\varphi$ tends to be zero. When the time constant $\tau = 0.13$ μs, the voltage difference $\Delta\varphi$ reaches the maximum.

Therefore, when the system time constant $\tau = 0.13$ μs, by adjusting the peak voltage of the system response, the voltage of the machining area could be higher than the decomposing voltage of the workpiece, while the voltage of the non-machining region far from the electrode is lower than the decomposing voltage. Thus, the localization of micro ECM could be the best.

III. CONTROL EQUATIONS AND PULSE WIDTH TUNING BASED ON QUADRATIC DIFFERENTIAL CIRCUITS

In order to further improve the machining accuracy, the second differential circuit is introduced to further shorten the peak time of the system response. On the basis of the machining technology with the first differential circuit, the quadratic differentiation of the pulse signals from the signal generator is completed. The equivalent circuit of the micro-ECM system is shown in Fig. 5 (time constant $\tau_1 = R_1C_1$, $\tau_2 = R_2C_2$).

Using Eq. (22), the step responses of the system are simulated. In order to improve the localization of micro-ECM, the time constant of $\tau_1 = \tau_2 = 0.13$ μs is used. The step responses of the first and second differential circuits are given in Fig. 6a. It shows:

The peak response time of the micro-ECM system with the first differential circuit is 200 ns, while the peak response time with the second differential circuit is 96 ns. With the increase of differential times, the peak system response time is shortened. At the same time, the peak voltage of the response will be greatly reduced, which also needs to be corrected by tuning the output voltage of the pulse power supply.

According to the above equation, the response voltage peak of the micro-ECM system with the secondary differential circuit can also be modified, and the minimum modified factor K of the pulse power supply can be obtained. Here, we still take the decomposing voltage of the workpiece to be

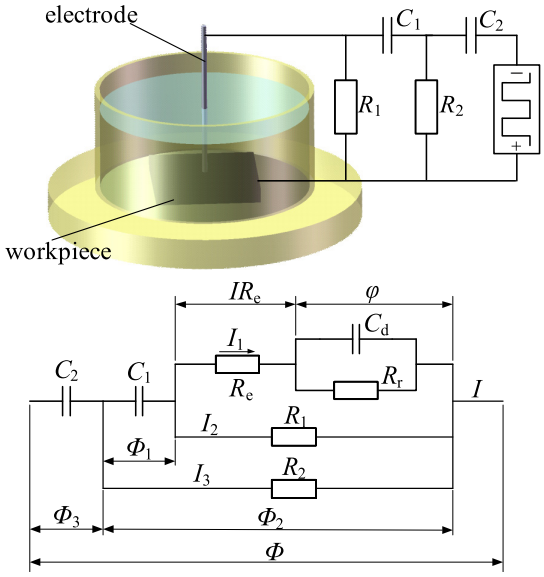

FIGURE 5. Equivalent circuit of the micro ECM system based on quadratic differential circuit.

$\varphi_d = 0.85$ V, and then

$$K' = \frac{\varphi_d}{\varphi_{\max}} = 8.85$$

The step response of the modified system is shown in Fig. 6b. It shows:

The modification of peak voltage has no effect on the response time. Therefore, the pulse width of the system response can be adjusted by controlling the differential times, while the peak voltage of the system response can be adjusted by modifying the output voltage of the pulse power supply for the micro-ECM technology based on the differential circuit.

IV. TEST

Based on the above analysis, the experiment of the ECM based on differential circuits is done. The electrolyte is H_2SO_4 solution with concentration of 0.05mol/L and the tool electrode is tungsten wire 10 μ m in diameter. The circuit of the micro ECM system after introducing the quadratic differential and rectifying circuits is shown in Fig. 7. In the half-wave rectifier circuit, the rectifier diode D is Schottky diode 1N5822, the forward on-voltage is 0.52V, the reverse breakdown voltage is 40V, and the resistance R' is 80 Ω. The time constants of the two order differential circuits are both 0.13 μ s, in which the capacitance is $C_1 = C_2 = 0.01\mu$F and the resistance is $R_1 = R_2 = 13\Omega$.

Using the system, we produced some micro-structures on the nickel film (see Fig. 8). The pulse signal frequency was 100 kHz, the duty cycle was 50%, and the pulse peak voltage was 10.86 V.

For machining a micro-cantilever beam, the width of the machining slot was 11.13 μm, and the machining clearance between the tool and the workpiece was only 565 nm.

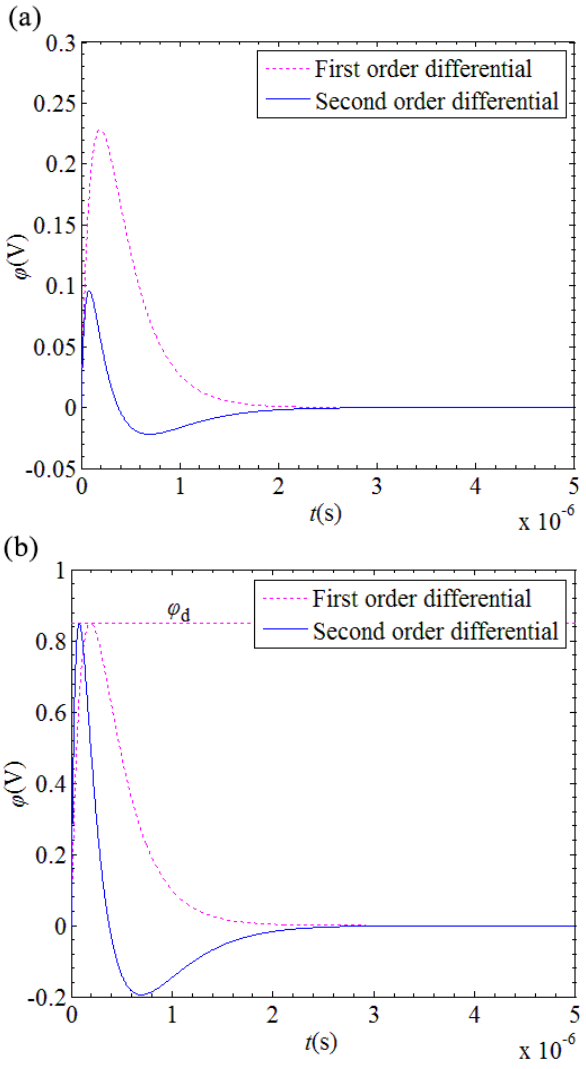

FIGURE 6. Step responses for different differential times before and after modification. a) before modification; b) after modification.

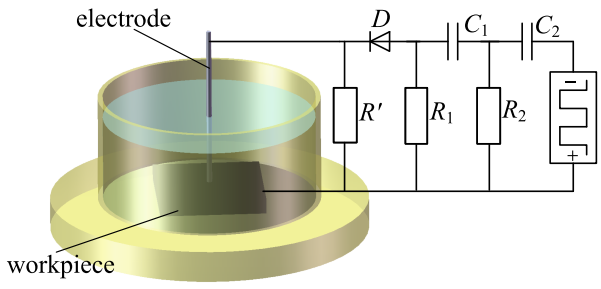

FIGURE 7. Diagram of the electrochemical machining based on differential circuits.

For the micro-curved beam, the width of the spiral groove was 11.037 μm, and the machining clearance between the tool and the workpiece was 519 nm.

The above results show that the micro-structure obtained using our machining system has little stray corrosion, uniform groove widths, and flat micro-groove edges. The machining

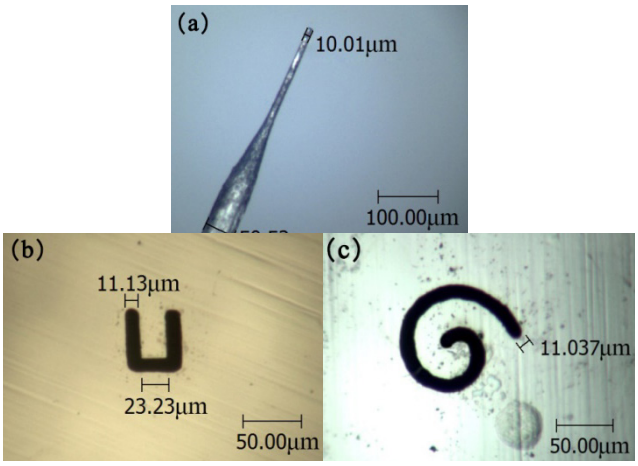

FIGURE 8. Machined micro-structures. a) tool electrode; b) micro-beam machined; c) micro-curved beam.

clearance reaches nanometer level. It illustrates our mathematical model for tuning pulse width of the voltage signals by means of the differential circuits in the micro-ECM.

Using conventional circuit, if the pulse signal frequency is 100 kHz, the duty cycle is 50% (pulse width is 5μs), the machining clearance between the tool and the workpiece is 42μm. For conventional circuit, in order to increase machining accuracy, only effective way is increasing pulse signal frequency (reduce pulse width). In [17], using 50 ns pulse width voltage, and the machining accuracy is 2 μm. Using our novel circuit, if the pulse signal frequency is still 100 kHz, and the duty cycle is 50% (pulse width is 5μs), the machining clearance between the tool and the workpiece gets to about 500nm (without using expensive nanosecond pulse power source).

The precision using our method reaches nanometer order of magnitude, and the machining accuracy is much higher than that of using 50 ns pulse width voltage in reference [17] (it is 2 μm). Compared with the conventional circuit, the accuracy of the new method is improved by about 80 times under the same pulse width. Compared with the nanosecond pulse power source, the accuracy increased about 4 times.

V. CONCLUSION

The present study proposed a mathematical model for tuning pulse width of the voltage signals by means of the differential circuits in electrochemical micro machining. Using the model, the step responses of the system under different time constants were simulated, which showed that the pulse width of the step response becomes quite short when the time constant of the differential circuit is short enough. Based on it, stray corrosion in ECM was investigated and the system time constant corresponding to the best localization of micro ECM was determined. Based on the model, an electrochemical micro machining system was produced. Using this system, some micro-structures were successfully

produced. The machining accuracy reaches nanometer scale. This illustrates our mathematical model for electrochemical micro machining with differential circuits.

REFERENCES

[1] L. Wu, J. Wang, Y. Shen, L. Liu, and J. Xi, "Electrochemical evaluation methods of vanadium flow battery electrodes," *Phys. Chem. Chem. Phys.*, vol. 19, no. 22, pp. 14708–14717, May 2017.

[2] B. E. Logan and K. Rabaey, "Conversion of wastes into bioelectricity and chemicals by using microbial electrochemical technologies," *Science*, vol. 337, no. 6095, pp. 686–690, Aug. 2012.

[3] P. Bataillard, F. Gardies, N. Jaffrezic-Renault, C. Martelet, B. Colin, and B. Mandrand, "Direct detection of Immunospecies by capacitance measurements," *Anal. Chem.*, vol. 60, no. 21, pp. 2374–2379, Nov. 1988.

[4] C. H. Luo and Y. Rudy, "A dynamic model of the cardiac ventricular action potential. I. Simulations of ionic currents and concentration changes.," *Circulat. Res.*, vol. 74, no. 6, pp. 1071–1096, Jun. 1994.

[5] M. Kock, V. Kirchner, and R. Schuster, "Electrochemical micromachining with ultrashort voltage pulses—A versatile method with lithographical precision," *Electrochimica Acta*, vol. 48, nos. 20–22, pp. 3213–3219, Sep. 2003.

[6] C. J. Mcneil, D. Athey, M. Ball, W. O. Ho, S. Krause, R. D. Armstrong, J. Des Wright, and K. Rawson, "Electrochemical sensors based on impedance measurement of enzyme-catalyzed polymer dissolution: Theory and applications," *Anal. Chem.*, vol. 67, no. 21, pp. 3928–3935, Nov. 1995.

[7] A. Gebbert, M. Alvarez-Icaza, W. Stoecklein, and R. D. Schmid, "Real-time monitoring of immunochemical interactions with a tantalum capacitance flow-through cell," *Anal. Chem.*, vol. 64, no. 9, pp. 997–1003, May 1992.

[8] J. Kim, "A novel input-parasitic compensation technique for a nanopore-based CMOS DNA detection sensor," *J. Korean Phys. Soc.*, vol. 69, no. 11, pp. 1705–1710, Dec. 2016.

[9] K. Yagiuda, A. Hemmi, S. Ito, Y. Asano, Y. Fushinuki, C.-Y. Chen, and I. Karube, "Development of a conductivity-based immunosensor for sensitive detection of methamphetamine (stimulant drug) in human urine," *Biosensors Bioelectron.*, vol. 11, no. 8, pp. 703–707, Jan. 1996.

[10] N. Jaffrezic-Renault and S. Dzyadevych, "Conductometric microbiosensors for environmental monitoring," *Sensors*, vol. 8, no. 4, pp. 2569–2588, Dec. 2008.

[11] M.-T. Von Srbik, M. Marinescu, R. F. Martinez-Botas, and G. J. Offer, "A physically meaningful equivalent circuit network model of a lithium-ion battery accounting for local electrochemical and thermal behaviour, variable double layer capacitance and degradation," *J. Power Sour.*, vol. 325, pp. 171–184, Sep. 2016.

[12] Y. F. Pulido, C. Blanco, D. Anseán, V. M. García, F. Ferrero, and M. Valledor, "Determination of suitable parameters for battery analysis by Electrochemical Impedance Spectroscopy," *Measurement*, vol. 106, pp. 1–11, Aug. 2017.

[13] E. Din, C. Schaef, K. Moffat, and J. T. Stauth, "A scalable active battery management system with embedded real-time electrochemical impedance spectroscopy," *IEEE Trans. Power Electron.*, vol. 32, no. 7, pp. 5688–5698, Jul. 2017.

[14] M. Meyer, L. Komsiyska, B. Lenz, and C. Agert, "Study of the local SOC distribution in a lithium-ion battery by physical and electrochemical modeling and simulation," *Appl. Math. Model.*, vol. 37, no. 4, pp. 2016–2027, Feb. 2013.

[15] E. Calzado, H. Schinca, L. Cabrales, F. García, P. Turjanski, and N. Olaiz, "Impact of permeabilization and pH effects in the electrochemical treatment of tumors: Experiments and simulations," *Appl. Math. Model.*, vol. 74, pp. 62–72, Oct. 2019.

[16] E. M. Calzado, J. L. G. Rodríguez, L. E. B. Cabrales, F. M. García, A. R. S. Castañeda, I. M. G. Delgado, L. M. Torres, F. V. G. Uribazo, M. M. González, S. C. A. Brooks, T. R. González, E. J. R. Oria, L. L. B. Roger, H. E. H. Figueroa, and G. D. Pèrez, "Simulations of the electrostatic field, temperature, and tissue damage generated by multiple electrodes for electrochemical treatment," *Appl. Math. Model.*, vol. 76, pp. 699–716, Dec. 2019.

[17] R. Schuster, "Electrochemical micromachining," *Science*, vol. 289, no. 5476, pp. 98–101, Jul. 2000.

[18] J. J. Maurer, J. J. Mallett, J. L. Hudson, S. E. Fick, T. P. Moffat, and G. A. Shaw, "Electrochemical micromachining of hastelloy B-2 with ultrashort voltage pulses," *Electrochimica Acta*, vol. 55, no. 3, pp. 952–958, Jan. 2010.

[19] V. Kirchner, L. Cagnon, R. Schuster, and G. Ertl, "Electrochemical machining of stainless steel microelements with ultrashort voltage pulses," *Appl. Phys. Lett.*, vol. 79, no. 11, pp. 1721–1723, Sep. 2001.

[20] B. Kim, C. Na, Y. Lee, D. Choi, and C. Chu, "Micro electrochemical machining of 3D micro structure using dilute sulfuric acid," *CIRP Ann.*, vol. 54, no. 1, pp. 191–194, 2005.

[21] H. S. Shin, B. H. Kim, and C. N. Chu, "Analysis of the side gap resulting from micro electrochemical machining with a tungsten wire and ultrashort voltage pulses," *J. Micromech. Microeng.*, vol. 18, no. 7, Jul. 2008, Art. no. 075009.

[22] J. A. Kenney and G. S. Hwang, "Electrochemical machining with ultrashort voltage pulses: Modelling of charging dynamics and feature profile evolution," *Nanotechnology*, vol. 16, no. 7, pp. S309–S313, Jul. 2005.

[23] N. Smets, S. Van Damme, D. De Wilde, G. Weyns, and J. Deconinck, "Time-averaged concentration calculations in pulse electrochemical machining, spectral approach," *J. Appl. Electrochem.*, vol. 39, no. 12, pp. 2481–2488, Dec. 2009.

[24] K. Sandeep and D. Akshay, "Fabrication of microchannels using rotary tool micro-USM: An experimental investigation on tool wear reduction and form accuracy improvement," *J. Manuf. Processes*, vol. 32, pp. 802–815, Apr. 2018.

[25] S. M. H. Darwish, N. Ahmed, and M. Abdulrahman Al-Ahmari, "Laser beam micro-milling of micro-channels in aerospace alloys," in *Advanced Structured Materials*. [Online]. Available: https://link.springer.com/book/10.1007%2F978-981-10-3602-6

[26] N. Ahmed, S. Anwar, K. Ishfaq, M. Rafaqat, M. Saleh, and S. Ahmad, "The potentiality of sinking EDM for micro-impressions on Ti-6Al-4V: Keeping the geometrical errors (axial and radial) and other machining measures (tool erosion and work roughness) at minimum," *Sci. Rep.*, vol. 9, Nov. 2019, Art. no. 17218.

[27] C. Chen, J. Li, S. Zhan, Z. Yu, and W. Xu, "Study of micro groove machining by micro ECM," *Procedia CIRP*, vol. 42, pp. 418–422, 2016.

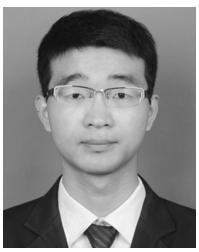

CHUANJUN ZHAO received the Ph.D. degree in mechanical engineering from Yanshan University, Qinhuangdao, China, in 2019.

His research interests include the electrochemical micromachining, MEMS control technology, and fabrication of micro or nanostructured structure.

LIZHONG XU received the Ph.D. degree in machine design and theory from Yanshan University, China, in 1999.

He is currently a Professor of machine design and theory with Yanshan University. His primary research interests are in the area of mechanical transmission, electromagnetic railgun, micro sensors, micro motors, and electromechanical integrated systems.